JOURNAL OF CATALYSIS 17, 277–286 (1970)

Oxidation of Zinc Sulfide Pellets

Application of a Model of Diffusion with Simultaneous Reaction Under Effective Diffusivity and Surface Area Profiles

E. MENDOZA,* R. E. CUNNINGHAM, AND J. J. RONCO

Departamento de Ingeniería Química and Departamento de Tecnología Química, Universidad Nacional de La Plata, La Plata, Argentina

Received February 28, 1969

The oxidation of spherical pellets of zinc sulfide obtained by compaction was studied. The temperature range was 1030 to 1334°K and though it can be accepted that temperature is uniform through the zinc sulfide pellet, it varies with time. In order to predict the experimental results, a previously developed model of diffusion with simultaneous reaction was applied. This model takes into account the existence of effective diffusivity and surface area profiles through the pellet and it is quantitatively stated by a correction factor of the Thiele modulus, the latter being calculated for the original effective diffusivity and surface area of the zinc sulfide pellet. Since the model was originally developed for isothermal conditions, the temperature variation was interpolated in the calculations. The calculated conversion-time relationship agrees satisfactorily with the experimental one. On the other hand, the calculated conversion-time from the moving boundary model differs very much as compared with the experimental one.

NOMENCLATURE

A	oxygen
a	surface area of solid B, L^2
a^+	dimensionless surface area of solid B, $a^+ = a/a_0$
B	zinc sulfide
b, c, d	stoichiometric coefficients, $b = c = d = \frac{2}{3}$
c	molar concentration, moles/L^3
C	sulfur dioxide
$c_A{}^+$	dimensionless concentration of A, $c_A{}^+ = c_A/c_{A_e}$
$c_B{}^+$	dimensionless concentration of B, $c_B{}^+ = c_B/c_{B_e}$
D	zinc oxide
$D_{eff_A}{}^B$	effective diffusivity of A in B, L^2/θ
$D_{eff_A}{}^D$	effective diffusivity of A in D, L^2/θ
$D_{eff_A}{}^{B,D}$	effective diffusivity of A in B with a gradient of D, L^2/θ
D^0	molecular diffusivity, L^2/θ
d_p	particle diameter, L
E	activation energy, Q/mole
F	coefficient in Eq. (B.1), defined in Eq. (B.2)
f	roughness factor
h^+	correction factor to the Thiele modulus
h_B	Thiele modulus for the initial zinc sulfide conditions of surface area and effective diffusivity
i	reaction components and inerts present in the pellet
ΔH	enthalpy of reaction, Q/mole
k	reaction rate coefficient per unit volume, moles of B/$L^3 \cdot p^{1/2}$
k'	reaction rate coefficient per unit surface area, moles of B/$L^2 \cdot p^{1/2} \cdot \theta$
L	characteristic length, $L = V/S$, L
m	generalized Thiele modulus, $m = h_B/h^+$
N	molar flux, moles/L^2
n	number moles, moles
p	particle pressure, p

* Present address: Facultad de Ingeniería en Petróleo, Universidad Nacional de Cuyo, Mendoza, Argentina

r	reaction rate per unit volume moles/$L^3 \cdot \theta$
r'	reaction rate per unit surface area, moles/$L^2 \cdot \theta$
R	radius, L
R_g	gas constant, pL^3/T mole
S	cross section, L^2
S^o	outer surface area of solid B, $S^o = S(f\epsilon_B)_s, L^2$
T	temperature, T
t	time, θ
V	volume, L^3
x	conversion
y	coordinate, $y = R_e - R_s$, L
z	distance, L

Subscripts

e	gas–solid D interface
i	internal
0	initial value
obs	observed
s	solid B-solid D interface

Greek Symbols

α	ratio of outer to total surface area of solid B, $= S^o/(S_i + S^o)$
γ	order of reaction
δ	dimensionless number defined in Eq. (A.2)
ϵ	voidage
ϵ_B	surface fraction of solid B
η	overall effectiveness factor
η_i	internal effectiveness factor
λ_{eff}	effective thermal conductivity
Ω	labrinth factor
$\nabla\cdot$	divergence
∇	gradient

Introduction

Let us consider the isothermal reaction

$$A_{(g)} + bB_{(s)} = cC_{(g)} + dD_{(s)}. \quad (1)$$

The rate of consumption of solid B is given by

$$-\frac{dn_B}{dt} = br_{A_s}\eta V, \quad (2)$$

where η is the overall effectiveness factor (OEF) which implies the internal as well as the external surface of solid B; it is described in another paper (*7*) and defined as follows:

$$\eta = r_{A_{obs}}/r_{A_s} = (1 - \alpha)\left(\frac{\alpha}{1 - \alpha} + \eta_i\right). \quad (3)$$

It is very difficult to obtain a solution for the OEF in terms of the kinetic and diffusional parameters of the system because it is necessary to solve differential equations with variable coefficients in order to get the internal effectiveness factor (IEF).

The IEF will arise from the composition field of A inside B which in turn is going to be calculated from the equations of change for A and B:

$$\epsilon\frac{\partial c_A}{\partial t} = \nabla \cdot D_{eff_A}{}^{B,D}\nabla c_A - r_A, \quad (4)$$

$$-\frac{\partial n_B}{\partial t} = br_{A_s}\eta V, \quad (5)$$

where

$$r_A = k'af(c_A) \quad (6)$$

$$D_{eff_A}{}^{B,D} = f(\epsilon,\Omega); \quad (7)$$

that is to say, the consumption of solid B produces a field of surface area of B and of effective diffusivity through it. This is the reason why Eqs. (4) and (5) are variable coefficient ones as stated in Eqs. (6) and (7).

However, with some simplifying assumptions it is possible to obtain a solution of Eqs. (4) and (5) even when the variation of the said coefficients is accepted. This has been done elsewhere (*8*) for a spherical solid with a first-order irreversible reaction with respect to A and provided the pseudo-steady state has been reached; the last assumption has been discussed for gas–solid reactions (*5*).

To get the said solution it was necessary to accept that the following relationship exists between the dimensionless molar concentrations of A and B:

$$c_A{}^+ = 1 - c_B{}^+, \quad (8)$$

which in fact is rigorously true when the reaction is zero order with respect to B and the Thiele modulus is very high (*2, 13*).

$$D_{eff_A} = D_A{}^0\epsilon^2. \quad (9)$$

In turn, once a pore pattern has been accepted, there is a relationship

$$a^+ = a^+(c_B{}^+). \quad (10)$$

Equations (8), (9), and (10) enable us to separate Eqs. (4) and (5) as independent ones and to express Eq. (4) in terms of c_A only.

Thus, Eq. (4) can be integrated if is accepted that the gaseous reactant A exhausts inside the solid B; this integration is performed to get the generalized Thiele modulus m (*6*) such that

$$\eta_i = 1/m, \tag{11}$$

where the generalized Thiele modulus is given by $m = h^+/h_B$, h^+ being a correction factor because of the existence of effective diffusivity and surface area profiles. This correction factor depends only upon the pore pattern and the original voidages of solids B and D. The value of h^+ was calculated for two pore patterns which do not allow new pores to be generated during the reaction: one pattern is that of a porous solid obtained by compaction of nonporous particles, and the other one is that of a network of cylindrical pores randomly interconnected (*14*).

The objective of this study was to verify the applicability of the development which we refer to as the moving layer model (MLM), to distinguish it from the well-known moving boundary model (MBM).

In order to achieve this, it is necessary to study a gas–solid reaction under the conditions which were previously accepted for that development and to calculate the conversion-time relationships and compare them with the experimental ones.

Fundamentals

The reaction. The oxidation of zinc sulfide was selected. This reaction can be expressed as

$$\tfrac{3}{2}O_2 + ZnS = SO_2 + ZnO. \tag{12}$$

So, it can be represented by Eq. (1) with $b = c = d = \frac{2}{3}$.

The kinetics of this reaction have been studied for zinc sulfide crystals (*10*), and the following rate equation was obtained:

$$r'_B = k' p_A^{\gamma}, \tag{13}$$

where

$$k' = 3.2 \times 10^{-3} e^{-50\,400/R_g T}, \frac{\text{mole ZnS}}{\text{cm}^2\ \text{atm}^{0.5}\ \text{sec}}, \tag{14}$$

$$\gamma = 0.5.$$

Two problems arise when selecting this reaction: the reaction rate is nonlinear with respect to A and, because of the high heat of reaction, the isothermal conditions are difficult to achieve.

The first trouble implies only that no analytic solution is available. On the other hand, the second one is more serious because it implies the necessity of writing the thermal energy balances for the system. First of all, however, it is important to remember that the isothermal conditions imply uniformity as well as constancy of temperature in the system. We must then analyze both separately.

The problem of the temperature uniformity is analyzed in Appendix A where it is shown that the temperature can be accepted as being uniform though solid B. Hence, only the problem of the time variation of temperature remains. This is discussed in the statement of the equations of the problem.

The equations of change. When the gaseous reactant exhausts inside the solid, the following relationship holds (*6*):

$$-(dp_A/dz)_s = L_s r_{A_s}/(D_{eff_A}{}^D/R_g T_s)m. \tag{15}$$

Equation (15) is valid for the instantaneous value of the uniform temperature T_s.

If the value of h_B is introduced in the generalized Thiele modulus of Eq. (15), the following result arises:

$$-(dp_A/dz)_s = (D_{eff_A}{}^B/D_{eff_A}{}^D)h^+ \times \left[\frac{2}{\gamma+1}\frac{k}{b}\frac{(p_{A_s})^{\gamma+1}}{D_{eff_A}{}^B/R_g T_s}\right]^{0.5} \tag{16}$$

where $k = k'a$.

If we take into account that Eq. (2) can be written as

$$-\frac{dn_B}{dt} = r'_{B_g} S_s^o - b(D_{eff_A}{}^D/R_g T_s) S_s (dp_A/dz)_s, \tag{17}$$

by introducing Eq. (16) in (17) we obtain

$$-\frac{dn_B}{dt} = r'_{Bs}S_s^o - h^+S_s \times \left[\frac{2b}{\gamma+1}k'(D_{eff_A}{}^B/R_gT_s)(p_{A_s})^{\gamma+1}\right]^{0.5} \quad (18)$$

Equation (18) gives the consumption rate of solid B due to the reaction which takes place on its outer and internal surface areas.

It is seen though that the partial pressure of A at the solid B–solid D interface appears in Eq. (18). We must then relate it with that at the gas–solid interface. For that it is necessary to introduce the mass transfer rate of A through the ash layer:

$$N_A = 4\pi R_e^2 D_{eff_A}{}^D R_s \times (p_{A_e} - p_{A_s})/R_e(R_e - R_s)R_gT_s. \quad (19)$$

Eq. (20) is valid for spherical geometry. At the same time it is

$$N_A = -\frac{1}{b}\frac{dn_B}{dt} = \frac{1}{b}c_{B_0}\frac{d}{dt}V(1-\eta_i), \quad (20)$$

provided the pseudo-steady state has been reached.

If the reaction is first order with respect to A and isothermal, then the relationship between p_{A_s} and p_{A_e} can be derived immediately and the conversion-time relationship can be obtained by applying Eq. (2).

However, this is not our case. The solid temperature, though uniform, varies with time. Hence, we must apply the thermal energy balances:

$$\frac{d}{dt}(\Sigma c_i c_{pi})T_s = r_{A_s}(-\Delta H)\eta, \quad (21)$$

$$r_{A_s}(-\Delta H)\eta = \lambda_{eff}{}^D(T_s - T_e). \quad (22)$$

Consequently, it is necessary to obtain the relationship among p_{A_s}, R_s, and T_s from Eqs. (18), (19), and (2) and then to apply Eqs. (20) and (21) to calculate $x_B(t)$.

It is obvious that the introduction of Eqs. (20) and (21) complicates the calculations. Furthermore, if we take into account that the system could be in a geometric instability region (self-heating) and that the knowledge about the effective thermal conductive is not accurate, the introduction of Eqs. (20) and (21) could lead to an error. This kind of instability was experimentally observed for the zinc sulfide oxidation and theoretically analyzed by Cannon and Denbigh (*11*) and more recently and deeply by Beveridge (*3*). It is observed that this instability is to be expected, especially at the beginning of the reaction when the ash layer is beginning to grow. Consequently, a calculation error due to this instability will be accumulative for the rest of the run.

But besides this, it is important to keep in mind that the objective of this study was the experimental verification of a theoretical development. On the other hand, it is not our objective to demonstrate the applicability of Eqs. (18) to (22), which in fact are *a priori* correct.

The only verification regarding the fundamental equations of the system refers to the calculated numerical value of h^+. Hence, it will be important to intent to eliminate Eqs. (21) and (22) from the calculations or to replace them.

Thus, if the relationship $T_s(R_s)$ were available, it could be introduced in Eqs. (18) and (19) to get the relationship $p_{A_s}(R_s)$, which in turn would enable us to solve Eq. (21). The relationship $T_s(R_s)$ must be an experimental datum.

Therefore, if in the run in which the relationship $x_B(t)$ is to be measured the relationship $T_s(t)$ is also recorded, then the function $T_s(x_B)$ could be calculated. But since there is a relationship $x_B(R_s)$ given elsewhere (*8*) as:

$$1 - x_B = (V/V_0)(1-\eta_i), \quad (23)$$

we will be able to calculate T_s as a function of R_s. It is to be observed that this procedure only avoids the use of Eqs. (21) and (22) but it does not induce the final result at all.

To perform the proposed calculation, a set of parameters is necessary: (i) the reaction kinetics, Eqs. (13) and (14); (ii) the effective diffusivities of oxygen through zinc sulfide and zinc oxide, which are to be experimentally measured (Appendix C); and (iii) the numerical value of the correction factor h^+, which is to be calculated (Appendix B).

Experimental Part

Selection of reaction conditions. To select the reaction conditions, the previous experience of Denbigh (*12*) for the zinc sulfide pellets oxidation was taken into account. Denbigh studied the oxidation of 1.02-cm-diameter spherical zinc oxide pellets presintered at 1423°C in nitrogen atmosphere.

When the pellets were not presintered, the initial reaction rate varied with Reynolds numbers based upon pellet diameter ranging between 40 and 100.

On the other hand, for presintered pellets the initial reaction rate is lower and there is chemical control up to 1273°C. At temperatures higher than 1273°C, the influence of the mass transfer resistance of the boundary layer begins to appear, and at temperatures of 1573°C and higher, the oxidation of gaseous zinc sulfide is predominant.

If we take into account these results, it will be necessary to carry on the reaction below 1273°C at the same Reynolds number range with presintered pellets in order to avoid boundary layer effects.

Chemicals. The chemicals used were: zinc sulfide of high purity from B.D.H. and air as a source of oxygen.

The zinc sulfide powder screened between U. S. Tyler mesh 100 and 200 was compacted in spheres 1.01 cm in diameter. The compaction was performed in a mold which contained a Pt–Pt Rh 10% thermocouple with its junction in the center of the sphere and the two wires emerging in opposite directions. The compaction was performed at 3200–3500 kg/cm^2 pressure.

Equipment. The equipment is shown schematically in Fig. 1. Basically it consists of three parts, in which the following operations were performed:

1. Flow measurement, which was done by means of U-tube mercury flow meters. Two separate lines of gases were available, one of air and the other of nitrogen. Before entering the flow meters, the gases were dried with calcium chloride and silica gel.

2. Oxidation, which was carried out in the reactor. The reactor was a vertical oven electrically heated by silicon carbide resistors with a refractory tube $\frac{3}{4}$ in. in diameter and 40 cm in length. Two Pt–Pt Rh 10% thermocouples entered the reactor through the bottom and were placed inside two refractory sheaths. One thermocouple was pressed in the center of the sphere to serve as a support for the pellet; the other one was placed with its junction in the gas phase near the pellet surface. The signals of the two thermocouples were recorded continuously.

3. Gas analysis by potentiometric titration, which is described as follows. When sulfur dioxide bubbles in the iodine side of

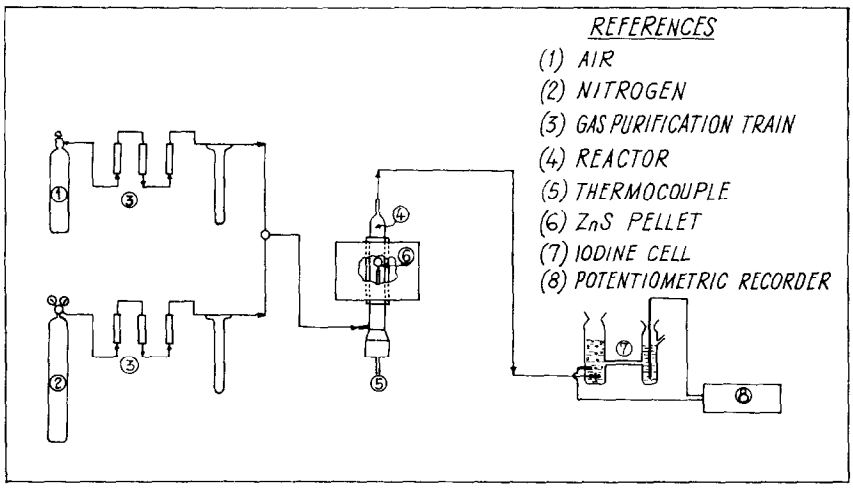

FIG. 1. Schematic diagram of equipment.

the cell, I_3^- is consumed. Hence, the potential variation of the cell measures the total amount of sulfur dioxide which was absorbed. The potential variation in a run was 6% of the initial value. In order to increase the sensibility, a potential equal to that of the cell was opposed to it. The calibration was performed by generating known amounts of sulfur dioxide obtained by decomposing a sodium thiosulfate solution with sulfuric acid. The cell signal was recorded continuously. The residence time of the gases between the pellet and the cell was about 0.01 sec.

Experimental Measurements

1. Reaction runs. Before the reaction the pellet was sintered by flowing nitrogen during 15–20 min at 1323°C. Temperature was then set at the desired value and the nitrogen stream was replaced by that of air; this was taken as the initial condition for the run. The zinc sulfide conversion and the temperature inside the pellet are shown as a function of time for four different runs in Fig. 2. Because of the very low residence time of the gases between the pellet and the cell, the effect of dispersion of the sulfur dioxide is negligible. Furthermore, exploratory runs showed the absence of boundary layer influence.

2. Properties of the solid phase. The BET specific surface of the sintered pellet was 260 cm^2/g. On the other hand, the pore size distribution and effective diffusivity of oxygen were determined for the zinc sulfide pellet and for zinc oxide obtained at two different temperatures. This can be seen in detail in Appendix C.

Calculations

Taking into account the calculation technique described before, the first part consists in the calculation of the $p_{A_s}(R_s)$ relationship. For that the radius of the pellet was divided in 50 increments. It was accepted that Eqs. (18) and (19) were equal when they differed in less than 10^{-8} mole/sec. The reason for the choice of that figure is based on a previous analysis of the convergence of p_{A_s} and R_s.

The relationship between p_{A_s} and R_s was obtained by trial and error by the method of Regula Falsi in a digital computer. The influence of temperature was computed interpolating the function $T_s(R_s)$ by the method described before. The calculation was interrupted when the asymptotic solu-

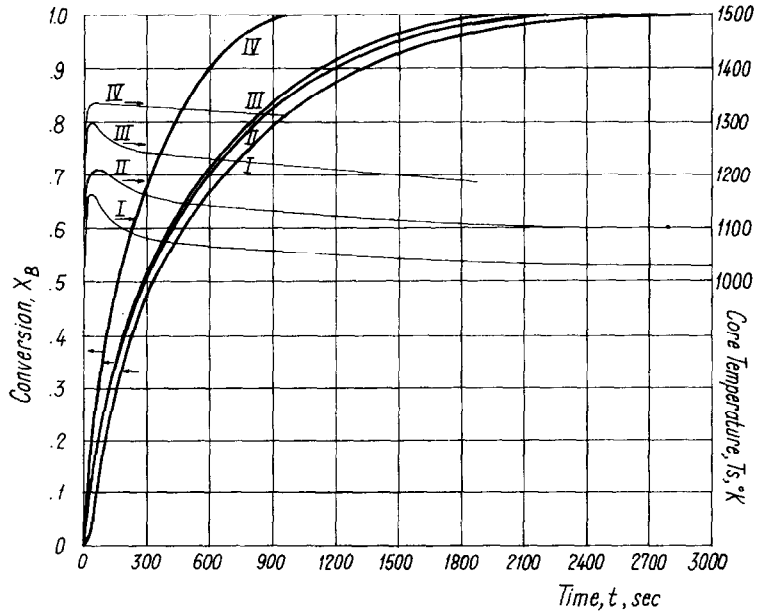

FIG. 2. Experimental results.

tion of the IEF was no longer valid. For the said calculation, the value of the reaction parameters were calculated from Eq. (14) and the effective diffusivities were taken from Table 1. It was accepted that $(f\epsilon_B) = 1$.

TABLE 1

Sample	Effective diffusivity of oxygen (cm^2/sec)			
	1000°K	1100°K	1200°K	1300°K
ZnS	0.21	0.24	0.28	0.32
ZnO (1073°K)	0.31	0.36	0.42	0.47
ZnO (1273°K)	0.53	0.62	0.71	0.81

Once this calculation is performed, the relationship between p_{A_s}, R_s, and r_B is available.

Now it is possible to apply the criterion for the validity of the moving boundary model (*9*). When the ratio $\alpha/(1 - \alpha)\eta_i$ was calculated for different values of R_s for the four runs, it ranged from 0.02 to 0.22. If we take into account that this ratio gives the quotient between the moles consumed on the outer surface area and those consumed on the internal one, it is seen that the system is very far from the moving boundary model.

Hence, we can come back to our calculation. The calculated relationship between r_B and R_s was represented by a polynom of the seventh degree which we will call $P(R_s)$, taking 100 pairs of values of r_B and R_s.

It was then possible to begin the second part of the calculation, which is the integration of Eq. (20). Equation (20) can be written as follows:

$$\frac{dt}{dy} = \frac{4\pi(R_c - y)^2}{[P(y)/c_B] + (d/dt)(V\eta_i)}, \quad (24)$$

if a new variable is defined as $y = R_0 - R_s$. Hence, the initial condition is given by $t = 0$, $y = 0$.

As the relationship $\eta_i V(t)$ is unknown, Eq. (24) was integrated in two steps, in both cases applying the Runge Kutta method of fourth order.

In the first step the $\eta_i V$ term of Eq. (24) was neglected and a first, approximated, relationship between t and y was calculated. With this relationship it was then possible to begin the second step. The function $\eta_i V(t)$ was calculated and then the $d(\eta_i V)/dt$ was calculated by increments. After this, Eq. (24) was integrated three times by successive approximations. The fourth integration gave a variation in the calculated time with respect to that of the third integration less than 0.5%.

Once Eq. (24) was integrated, the calculation of the function $x_B(t)$ was immediate. The calculated relationship between x_B and t in the first approximation (approximated moving layer model, AMLM) and after the fourth one (moving layer model, MLM) is shown in Figs. 3 to 6, together with the experimental results for the four runs. As shown, the calculated value approximates the experimental result in a wide range of conversion. It is also interesting to calculate $x_B(t)$, which would be obtained if the system would obey the moving boundary model (MBM). In such a case the calculation simplifies because now it is $\eta_i = 0$.

The rate of consumption of solid B can now be expressed by

$$-(dR_s/dt) = k'(p_A)^{0.5}/c_{B_0}. \quad (25)$$

Equalizing Eqs. (25) and (19) and reordering, the following result is obtained:

$$p_{A_s} = \left\{0.5\sqrt{\left[\frac{k'R_s(R_e - R_s)}{b(D_{eff_A}{}^D/R_gT_s)R_e}\right]^2 + 4p_{A_e}} - \frac{k'R_s(R_e - R_s)}{2b(D_{eff_A}{}^D/R_gT_s)R_e}\right\}^2. \quad (26)$$

Equation (25) can be integrated by successive approximations with the aid of Eq. (26) and interpolating the influence of temperature in the described way. The calculation was performed by means of the Regula Falsi method and by dividing the radius of the pellet into 50 increments.

The results are also shown in Figs. 3 to 6, which show that the calculated conversion-time relationship differs very much from the calculated one.

Another result of interest is that of the overall effectiveness factor variation during the run. This is shown in Fig. 7 for the four studied runs.

At the beginning of the run and as a

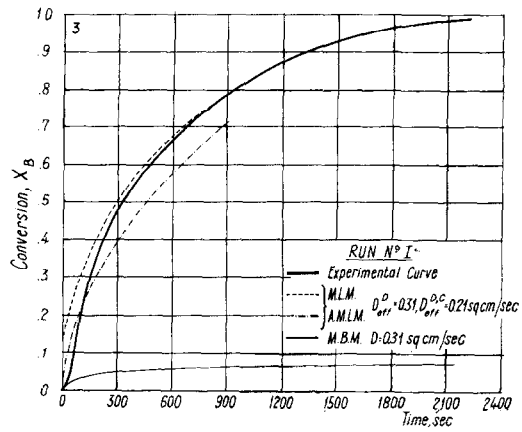

FIG. 3

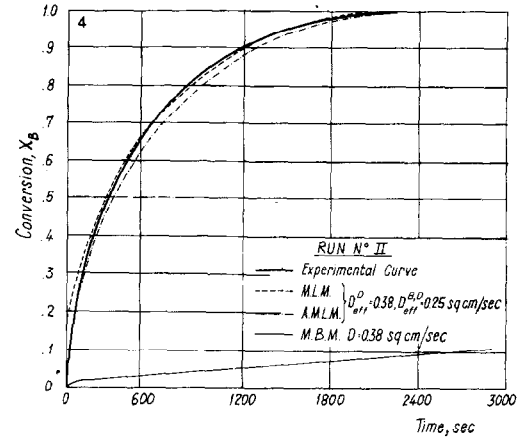

FIG. 4

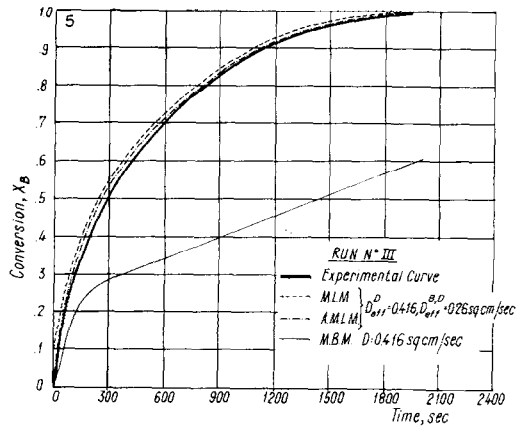

FIG. 5

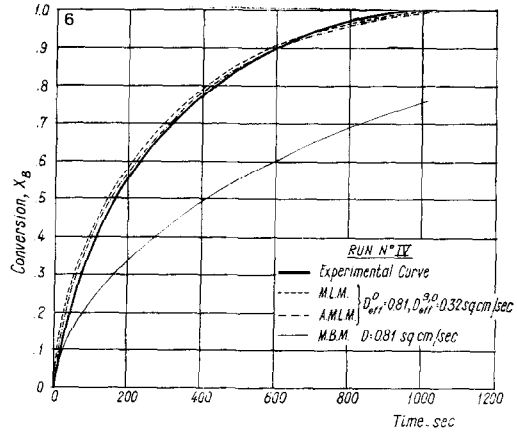

FIG. 6

FIGS. 3 to 6. Calculated vs. experimental results.

consequence of the ash layer formation, the effectiveness factor decreases very rapidly because it depends upon p_{A_s}. Later on, however, the effect of the decrease of the outer surface of the core per unit volume begins to prevail and so the effectiveness factor begins to increase. In Fig. 7, the m/R term has been left as a parametric variable; during the run the effectiveness factor would follow one of those curves of constant m/R if there would not be composition gradients through the ash layer.

CONCLUSIONS

It was verified that the oxidation of zinc sulfide pellets between 1030 and 1334°K takes place by means of diffusion with simultaneous chemical reaction inside the zinc sulfide pellet and with composition gradient through the zinc oxide layer. The experimental results can be predicted by applying a calculated correction factor to the Thiele modulus expressed in terms of the original surface area and effective diffusivity.

APPENDIX A: ISOTHERMAL CRITERION

The absence of temperature gradients can be checked applying the Anderson criterion (*1*). Nevertheless, it is necessary to know the experimental reaction rate in order to apply that criterion.

If the system is in the asymptotic region of the internal effectiveness factor (which is

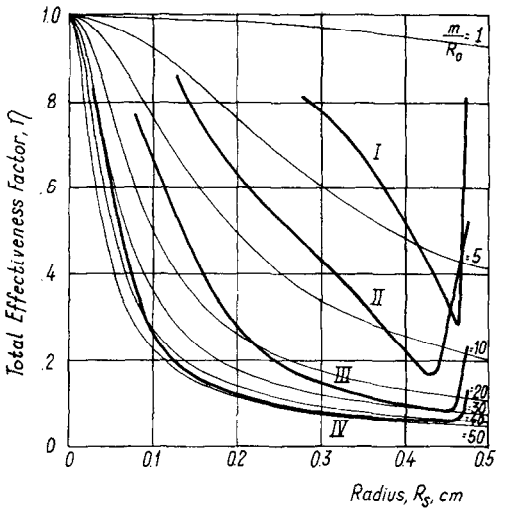

FIG. 7. Effectiveness factor variation during the runs.

the assumption made in the calculation of h^+), a boundary mark to the dimensionless group δ can be applied as developed by Petersen (*15*). Though Petersen established the boundary mark for a first-order reaction, it does not vary significatively for an order of 0.5; hence, we can say that whenever

$$-0.3 < \delta < 0.3, \qquad \text{(A.1)}$$

the isothermal effectiveness factor will differ less than 5% from the nonisothermal one.

If we take into account that it is

$$\delta = \frac{E(-\Delta H)D_{\mathrm{eff_A}^{B,D}}c_{A_s}}{R_g T_s^2 \lambda_{\mathrm{eff}}^{B,D}}, \qquad \text{(A.2)}$$

we can apply the criterion for limiting conditions, that is to say for the maximum value of $D_{\mathrm{eff_A}^{B,D}}c_{A_s}/T_s^2$, and we can calculate the value of the effective thermal conductivity which is necessary to achieve the isothermal behavior. The limiting conditions are those of the initial reaction.

If the calculation is performed for 1000°K ($D_{\mathrm{eff_A}^{B,D}} = 0.3$ cm²/sec), it must be

$$\lambda_{\mathrm{eff}}^{B,D} > 1.74 \times 10^{-4} \text{ cal/cm sec °K}, \qquad \text{(A.3)}$$

in order to achieve the absence of temperature gradients.

The value given in Eq. (A.3) corresponds to the thermal conductivity of nitrogen at 1000°K. Hence, the absence of temperature gradients inside the pellet can be accepted.

APPENDIX B: CALCULATION OF h^+

The calculation procedure of the correction factor h^+ has been given elsewhere (*8*). In this case the dispersed solid model has to be applied. So, for an irreversible reaction of 0.5 order it is

$$h^+ = \left[1.5 \int_0^1 (1 + Fc_A^+)^2 \times (1 - c_A^+)^{2/3}(c_A^+)^{0.5}\, dc_A^+ \right]^{0.5}, \qquad \text{(B.1)}$$

where

$$F = (\epsilon_D - \epsilon_B)/\epsilon_B. \qquad \text{(B.2)}$$

Hence, taking into account the values of the voidages from Fig. 8, the numerical integration of Eq. (B.1) leads to a value of

$$h^+ = 1.19. \qquad \text{(B.3)}$$

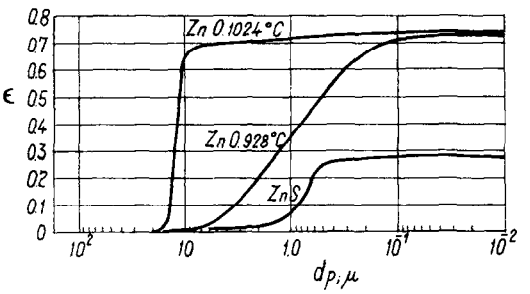

FIG. 8. Porosity and pore size distribution of unreacted and reacted samples.

APPENDIX C: PROPERTIES OF THE SOLID PHASE

1. Effective Diffusivities. Powdered zinc sulfide was compacted in cylindrical pellets 1.1 cm in diameter and 0.5 cm in height. These pellets were sintered in nitrogen atmosphere at 1323°C, and some of them were oxidized with air at 1073 and 1273°C.

The effective diffusivity of hydrogen in nitrogen was measured in a conventional diffusion cell at room temperature. The effective diffusivity of oxygen in nitrogen was calculated from these results applying the Chapman Enskog equation (*4*). The results are given in Table 1.

2. Macropore size distribution. The macropore size distribution was measured by the mercury penetration technique. The

results are shown in Fig. 8; it is interesting to see the pores opening in the zinc oxide due to the reaction.

References

1. Anderson, J. B., *Chem. Eng. Sci.* **18,** 147 (1963).
2. Ausman, J. M., and Watson, C. C., *Chem. Eng. Sci.* **17,** 323 (1962).
3. Beveridge, G. S. G., and Goldie, P. J., *Chem. Eng. Sci.* **23,** 913 (1968).
4. Bird, R., Stewart, W., and Lightfoot, E. N., "Transport Phenomena." Wiley, New York, 1960.
5. Bischoff, K. B., *Chem. Eng. Sci.* **18,** 711 (1963).
6. Bischoff, K. B., *AIChE J.* **11,** 351 (1965).
7. Calvelo, A., and Cunningham, R. E., *J. Catal.* **17,** 1 (1970).
8. Calvelo, A., and Cunningham, R. E., *J. Catal.* **17,** 1 (1970).
9. Calvelo, A., and Cunningham, R. E., *J. Catal.* **17,** 143 (1970).
10. Cannon, K. J., and Denbigh, K. G., *Chem. Eng. Sci.* **6,** 145 (1957).
11. Cannon, K. J., and Denbigh, K. G., *Chem. Eng. Sci.* **6,** 155 (1957).
12. Denbigh, K. G., and Beveridge, G. S. C., *Trans. Inst. Chem. Eng.* **40,** 23 (1962).
13. Ishida, M., and Wen, C. Y., *AIChE J.* **14,** 311 (1968).
14. Petersen, E. E., *AIChE J.* **3,** 443 (1957).
15. Petersen, E. E., "Chemical Reaction Analysis" Prentice-Hall, Englewood Cliffs, N. J., 1965.